THE ASTROPHYSICAL JOURNAL, 420:33–43, 1994 January 1

A MEASUREMENT OF THE HUBBLE CONSTANT FROM THE X-RAY PROPERTIES AND THE SUNYAEV-ZEL'DOVICH EFFECT OF ABELL 2218

M. BIRKINSHAW AND J. P. HUGHES
Harvard-Smithsonian Center for Astrophysics, 60 Garden Street, Cambridge, MA 02138
Received 1993 February 8; accepted 1993 July 13

ABSTRACT

The distance of the cluster of galaxies Abell 2218, and hence the value of the Hubble constant, has been measured by comparing the X-ray properties and the Sunyaev-Zel'dovich effect of the cluster. The result for the Hubble constant is $H_0 = 65 \pm 25$ km s^{-1} Mpc^{-1}, where the error includes the random and systematic errors, combined in quadrature, and the largest contributions to the overall error come from systematic errors in the Sunyaev-Zel'dovich effect data and in the X-ray spectrum of the cluster. The X-ray and Sunyaev-Zel'dovich effect data are consistent with the same model for the intergalactic medium in Abell 2218 (an isothermal β-model with $\beta \approx 0.65$ and cluster core radius $\approx 1'.0$). A previous report of a smaller Hubble constant, found by applying the same method on the same cluster, is shown to be based on a model for the cluster gas that is inconsistent with the *Einstein* IPC data. The present result for the Hubble constant is consistent with the value found earlier for the cluster Abell 665: by combining the results of the method for both clusters we conclude that the value of the Hubble constant is $H_0 = 55 \pm 17$ km s^{-1} Mpc^{-1}.

Subject headings: cosmic microwave background — cosmology: observations — distance scale — galaxies: clusters: individual (Abell 2218) — X-rays: galaxies

1. INTRODUCTION

The uncertainty in the value of the Hubble constant ($H_0 =$ 50–100 km s^{-1} Mpc^{-1}) reflects not the quoted errors on the values estimated by different workers, but rather the spread of those independent estimates. Since the spread of values is much wider than the typical errors quoted, there remain large, unrecognized, systematic errors in some or all of the published values. Under these circumstances, a variety of nonstandard ("astrophysical") approaches have been used in the attempt to measure H_0. These methods derive distances for distant objects directly, from an understanding of the physics responsible for the observed properties of those objects. Among these models is one that measures the distance of a cluster of galaxies by comparing its X-ray emission, which is the thermal radiation from hot gas in the cluster, with its Sunyaev-Zel'dovich effect, the reduction in the brightness of the microwave background radiation caused by inverse-Compton scattering by electrons in the hot gas (Gunn 1978; Silk & White 1978; Birkinshaw 1979; Cavaliere, Danese, & De Zotti 1979).

Recent improvements in the Sunyaev-Zel'dovich effect data (Birkinshaw, Gull, & Hardeback 1984; Uson 1987; Birkinshaw et al. 1993), and in the X-ray spectroscopy of the distant ($z > 0.1$) clusters of galaxies for which good Sunyaev-Zel'dovich effect scans have been measured (McHardy et al. 1990; Hughes & Tanaka 1992), have allowed this method of estimating the value of the Hubble constant to be used for two clusters of galaxies. For the first, Abell 665, Birkinshaw, Hughes, & Arnaud (1991) found $H_0 = (40 \text{ to } 50) \pm 12$ km s^{-1} Mpc^{-1} (including an assessment for possible systematic errors), which tends to support the long ($H_0 \approx 50$ km s^{-1} Mpc^{-1}) distance scale of the universe. For the second cluster, Abell 2218, McHardy et al. (1990) found $H_0 = 24^{+23}_{-10}$ km s^{-1} Mpc^{-1}. However, this estimate did not use the best recent Sunyaev-Zel'dovich effect data, and appears to have used an inconsistent modeling of the intracluster medium in deriving this value of H_0 (Birkinshaw et al. 1991). The purpose of the present paper is to reestimate the value of H_0 based on the data for Abell 2218, making use of the best recent Sunyaev-Zel'dovich effect data, and with a fully consistent treatment of the intracluster medium in Abell 2218.

Although the errors on measurements of the Hubble constant using this method are large ($\gtrsim 25\%$), the method is valuable since it can be applied directly at redshifts > 0.1. The more standard methods of measuring H_0, which are applied at redshifts < 0.03, are subject to large sampling errors from the small volume of the universe lying in this range of redshift. The importance of a global estimator of the Hubble constant is evident in the result of Turner, Cen, & Ostriker (1992) that even if all the galaxies with $z \lesssim 0.025$ were surveyed and used in an H_0 measurement, the 95% confidence range on the resulting value of H_0 would be 50–128 km s^{-1} Mpc^{-1} (if the true value of $H_0 = 80$ km s^{-1} Mpc^{-1}) because this volume represents too small a sample of the universe to average effectively over the gravitationally induced motions of the galaxies that it contains.

Abell 2218 lies at a redshift of 0.171 (Dressler & Spinrad 1993, private communication), and because of its richness (Abell richness class 4: Abell 1958) it has been well studied in the X-ray (by *Einstein* imaging, and *Ginga* spectroscopy; McHardy et al. 1990), in the optical (Dressler 1978a, 1978b; Dressler & Spinrad 1993, private communication), and in the Sunyaev-Zel'dovich effect (Birkinshaw 1990 and references therein; Birkinshaw et al. 1993). The center of the galaxy distribution in the cluster was found (Birkinshaw 1979) to be $16^h35^m37^s$, $+66°18'30''$ (B1950), with an error of about $30''$ in each coordinate, and the galaxy distribution does not appear to show strong subcondensations in position (Birkinshaw 1979) or velocity (Dressler & Spinrad 1993, private communication). The velocity dispersion of the cluster, $\sigma_z \approx$ 1350 km s^{-1} Mpc^{-1} (Dressler & Spinrad) is comparable with

that of other rich clusters and is consistent with the large gravitating mass required to confine a hot, X-ray-emitting, atmosphere.

In § 2 the data on Abell 2218 are reviewed, with particular emphasis on the critical systematic errors that may remain in the data. The X-ray images and Sunyaev-Zel'dovich effect data are fitted to models for the intracluster atmosphere in § 3, where a value for the Hubble constant is derived. Section 4 discusses the differences between the present treatment and that of McHardy et al. (1990), identifying the cause of the discrepancy in the H_0 estimates, and combines the new result for H_0 with that derived earlier for Abell 665 (Birkinshaw et al. 1991) to produce a best overall result.

2. THE DATA

2.1. *Sunyaev-Zel'dovich Effect Data*

Abell 2218 has been observed more frequently in the Sunyaev-Zel'dovich effect than has any other cluster, and in consequence the published results for Abell 2218 have often been used to illustrate the level of inconsistency in the independent measurements. However, the most recent measurements of the Sunyaev-Zel'dovich effect are in better agreement (see Birkinshaw 1990; Birkinshaw et al. 1993), which suggests that the current observational results are sufficiently reliable for strong astrophysical and cosmological conclusions to be based on the data.

The most extensive Sunyaev-Zel'dovich effect data for Abell 2218 are those of Birkinshaw et al. (1993). These data were obtained through several years of observation over the period 1983–1990 using the OVRO 40 m telescope at 20.3 GHz. In the "microwave background" configuration that was used, the 40 m telescope provides two 1.'78 FWHM beams separated by 7.'15 in azimuth. Data were taken using both beam-switching and position-switching in a seven-point scan down the declination axis and through the center of the cluster (taken from the galaxy-count result of Birkinshaw 1979). The details of the experimental method, and a discussion of the sources of both random and systematic error in the data, have been given by Birkinshaw et al. (1993), which should be consulted for a detailed discussion of the observations.

The data collected from the 40 m telescope during the best weather conditions were selected and averaged to produce the results given in Table 1 and plotted in Figure 1. Brightness temperature (ΔT_{RJ}) values are reported both with and without corrections for contaminating radio sources near Abell 2218: it can be seen that the magnitudes of these corrections are small (less than the errors on the measurements) at all points except point e, which lies 2′ north of the cluster center. The ΔT_{RJ} values represent the brightness temperature differences between points in the scan and reference arc regions (7.'15 distant from these points) which are sampled by the "OFF" positions in the beam- and position-switching scheme. The varying weights at which different parallactic angles within these arcs are sampled cause the ΔT_{RJ} values in Table 1 to be complicated functions of the underlying Sunyaev-Zel'dovich effect of Abell 2218.

The major contributions toward the systematic errors given in Table 1 are listed below. More complete descriptions of the sources of these errors and of the methods used to estimate their sizes are given in Birkinshaw et al. (1993), but some description of these errors is necessary here to elucidate later descriptions of the uncertainties underlying the value of the central Sunyaev-Zel'dovich effect in the cluster and the value of the Hubble constant. The most important sources of error are those that are coherent across the scan, and hence have large

TABLE 1

SUNYAEV-ZEL'DOVICH EFFECT DATA

Point	Coordinates (B1950) R.A.	Coordinates (B1950) Decl.	Uncorrected ΔT_{RJ} (μK)	Corrected ΔT_{RJ} (μK)	Systematic Error ΔT_{syst} (μK)
a	$16^h35^m37^s$	+66°11′30″	−125 ± 34	−105 ± 59	±17
b	$16^h35^m37^s$	+66°14′30″	−121 ± 40	−97 ± 34	±17
c	$16^h35^m37^s$	+66°16′30″	−178 ± 28	−176 ± 32	±19
d	$16^h35^m37^s$	+66°18′30″	−427 ± 30	−445 ± 33	±18
e	$16^h35^m37^s$	+66°20′30″	+279 ± 32	−80 ± 77	±33
f	$16^h35^m37^s$	+66°22′30″	−66 ± 59	−98 ± 53	±18
g	$16^h35^m37^s$	+66°25′30″	−106 ± 32	−89 ± 42	±17

NOTES:

(1) The uncorrected values of ΔT_{RJ} are those without source corrections of any kind, but with the data taken under conditions of bad weather removed. Only point e in the scan is affected by radio source contamination at a level greater than the error on the uncorrected ΔT_{RJ}; the dominant source at point e is source 16 of the Moffet & Birkinshaw 1989 survey.

(2) The corrected values of ΔT_{RJ} have been corrected for radio sources both near the points in the scan and for sources in the reference arcs about these points onto which the 40 m telescope's reference beams switch. Significant corrections for sources in the reference arcs occur for several points in the scan: where sources in the reference arcs contribute more than 100 μK to the signal, the contaminated data have been deleted in calculating the results in the table. The random errors quoted have been increased by a factor that takes account of the year-to-year discordance in the data (§ 2.1).

(3) The systematic errors are those attributable for each point individually (errors 3–5 of § 2.1) and are $\pm 1\,\sigma$ errors.

(4) In addition to these systematic errors, ΔT_{syst}, the overall zero level of the data shows a systematic error of -43 ± 25 μK (Birkinshaw et al. 1993), so that the net ΔT_{RJ} at point d, for example, is -402 ± 45 μK if all systematic errors are combined with the random error in quadrature.

(5) The overall scale of the brightness temperatures may be in error by a factor of 1.00 ± 0.06.

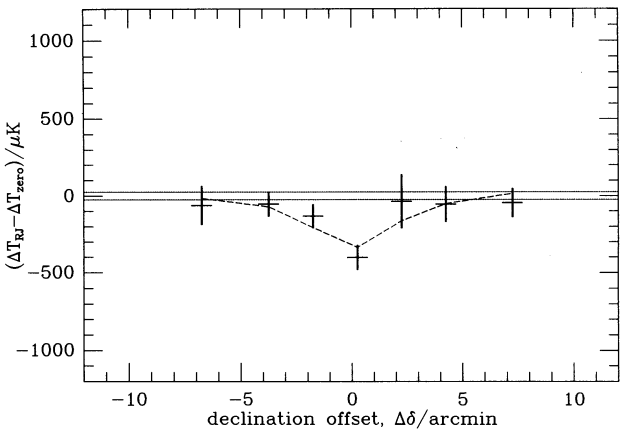

FIG. 1.—Sunyaev-Zel'dovich effect data for several points on an NS line through Abell 2218. The declination offsets for each point are measured relative to the cluster center deduced from the *Einstein* IPC image, of $16^h35^m42^s.8$, 66°18′44″.5 (B1950). The crosses at each point represent the microwave background radiation brightness temperature change, as measured with the OVRO 40 m telescope, including a contribution from systematic errors associated with that point (added in quadrature), and corrected for the zero level offset of −43 μK. The horizontal dotted lines indicate the ±25 μK error on this zero level offset. The brightness temperature scale is uncertain by ±6%. The dashed line represents the isothermal β model that best fits the X-ray data, adjusted to have the best normalization N_{RJ}.

effects on fits of models to the data.

1. The most serious of these errors is the uncertainty in the zero level of the scan, estimated to be -43 ± 25 μK (see Birkinshaw et al. 1993). This offset is represented by the dotted lines in Figure 1, and might be caused by differential spillover effects.

2. A second coherent error is caused by the uncertainty in the efficiency of the 40 m telescope, which causes the brightness temperature scale in Table 1 and Figure 1 to be uncertain by a factor 1.00 ± 0.06.

Systematic errors which are not coherent across the scan will in general have smaller effects on the parameters estimated by fitting models to the data, unless they appear at points with large "leverage" on those parameters. Into this class fall the following errors.

3. Errors caused by the uncertainty in the flux-density to brightness temperature conversion used in the correction for contaminating radio sources. The only significant error from this cause arises for point e (2′ north of the nominal cluster center) for which the measurement is contaminated by radio emission from Moffet & Birkinshaw (1989)'s source 16. A contribution of ±22 μK to the error in Table 1 has been assessed from this cause.

4. A significant contribution to the systematic error, of about ±16 μK, arises at each point because of the possibility that radio sources which were not detected in the Moffet & Birkinshaw (1989) survey might be affecting the apparent brightness in Table 1.

5. Where the Sunyaev-Zel'dovich effect of the cluster has a large gradient, or where the scan point lies near a radio source, small pointing errors in the telescope can cause significant variations in the detected signal. The size of this systematic error is estimated to vary from ±1 μK for source-free points far from the central Sunyaev-Zel'dovich effect peak in the cluster to ±20 μK for point e, where both the proximity of the radio source and the gradient in the Sunyaev-Zel'dovich effect contribute appreciably to the error.

6. The apparent random error for each point has also been increased by a factor to take account of the discordance in the data from year to year. This factor, which varies between 1.00 and 1.51, is intended to take some account of the variations in the data due to instrumental effects or other, unknown, effects, which varied from season to season of the observations.

Even when all these systematic errors are taken into account, the Sunyaev-Zel'dovich effect in Abell 2218 is clearly highly significant (Fig. 1), and strongly peaked near the center of the optical cluster. The apparent angular size of the Sunyaev-Zel'dovich effect in Figure 1 is about 2′ which is close to the FWHM of the 40 m telescope (1.′78)—the Sunyaev-Zel'dovich effect is not well resolved in these data. This does *not* imply that the FWHM of the Sunyaev-Zel'dovich effect from the atmosphere of Abell 2218 is about $(2^2 - 1.78^2)^{1/2} =$ 0.′9, since the beam-switching method of observing with the 40 m telescope causes components of the Sunyaev-Zel'dovich effect on angular scales greater than the beam-switching scale (7.′15) to be subtracted out. The structure of the atmosphere can be determined from these data only after careful fits that take the observational sampling explicitly into account: in general, the subtraction caused by the beam-switching causes the Sunyaev-Zel'dovich effect data to be less sensitive than the X-ray images to the overall structure of the atmosphere of Abell 2218.

2.2. *X-Ray Images*

Abell 2218 was observed by both imaging instruments on board the *Einstein Observatory*. The imaging proportional counter (IPC) imaged the cluster for 3398.6 s (live-time corrected exposure) on 1979 February 25. The high-resolution imager (HRI) was pointed toward Abell 2218 for 39283.3 s (live-time corrected exposure) on 1979 April 19. We utilize both of these data sets in our analysis. Although the IPC observation is relatively short, the cluster is clearly detected, and its surface brightness remains above the background level out to a radius of about 4.′5 from the cluster center. The HRI data are of higher angular resolution, but their usefulness in constraining the structural parameters of the diffuse cluster emission is limited by that instrument's higher intrinsic background and smaller effective area. In the HRI data, the X-ray surface brightness from A2218 exceeds the instrumental background only within a radius of about 40″ from the center of the cluster.

The IPC was a low-background gas-filled device capable of producing images (with spatial resolution of 36″) and spectra (with energy resolution $\Delta E/E \sim 1$ at 1 keV) in the 0.15–4.5 keV X-ray band. For the imaging analysis of Abell 2218 the range of observed photon energies was restricted to 0.8–3.5 keV (PI bins 5–10). This reduced the average level of the background (which contains a strong soft component) and decreased the sensitivity of the fitted electron number density in the cluster to the value of the line-of-sight hydrogen column density. Background was subtracted using the two standard background template maps: DSMAP, the sum of a large number of deep survey observations with bright sources removed, and BEMAP, an image of the bright Earth. The DSMAP was scaled to the Abell 2218 image using the ratios of the live times on the cluster and the deep surveys, and the remaining background was subtracted by scaling the BEMAP to the number of counts in the entire field of the image that lies more than 16′ from the cluster center (as described in detail in Birkinshaw, Hughes, & Arnaud 1991). The resulting image (using this

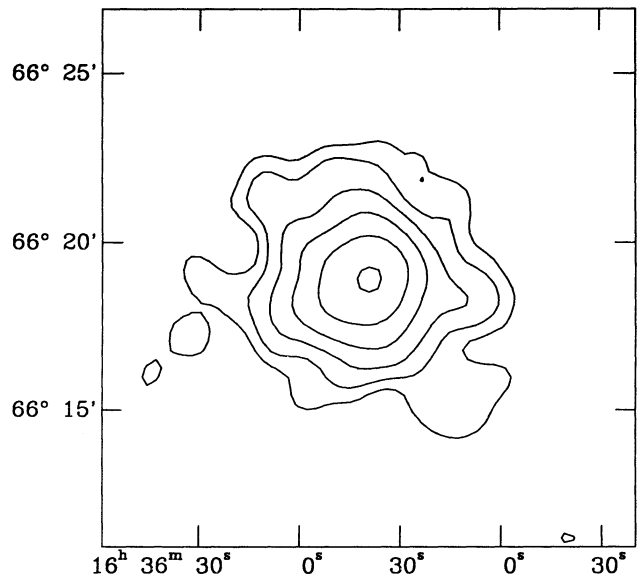

FIG. 2a

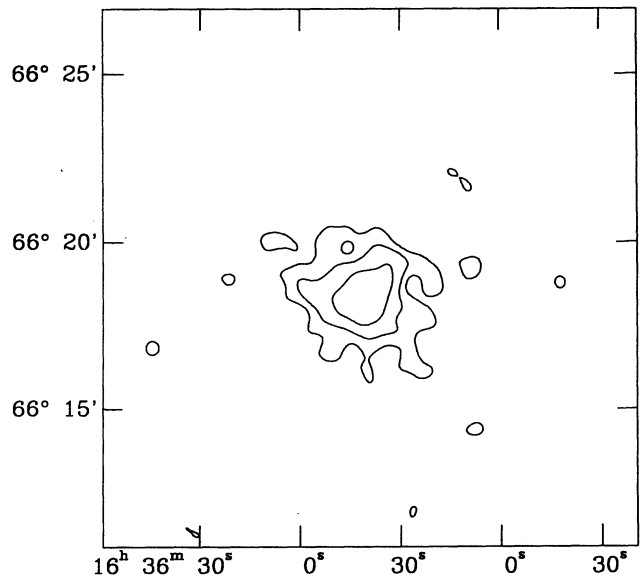

FIG. 2b

FIG. 2.—X-ray images of Abell 2218 from the *Einstein* IPC and HRI. (*a*) The IPC image, generated from the counts in the energy band 0.8–3.5 keV by convolution with a Gaussian of standard deviation 32″. The lowest contour corresponds to a value of 5.8×10^{-4} counts s^{-1} arcmin^{-2} which is 3 σ above the mean background level in the center of the field. Successively higher contour levels increase in logarithmic steps of 1.85. (*b*) The HRI image, generated from the counts by convolution with a Gaussian of standard deviation 16″. The lowest contour corresponds to a value of 1.2×10^{-3} counts s^{-1} arcmin^{-2} and successively higher contour levels increase in logarithmic steps of 1.85. The inner three contours shown for the HRI were chosen to correspond to the same X-ray brightness as the inner three contours of the IPC image (using the ratio of 3.05 IPC counts per HRI count, based on the best-fit spectral model). Apparent deviations from axisymmetry in this image are not statistically significant.

nominal background subtraction) is shown in Figure 2*a*, where Gaussian smoothing ($\sigma = 32''$) has been applied to the data to reduce statistical fluctuations. The effect of systematic errors in background subtraction was studied by varying the amount of the DSMAP subtracted by $\pm 20\%$ and redetermining the BEMAP scaling. Including an uncertainty caused by the errors in the background subtraction, the count rate of the cluster in 0.8–3.5 keV within a radius of 8′ of the center is 0.161 ± 0.009 s^{-1} (1 σ error).

The HRI was a micro-channel plate detector for broad-band imaging at high spatial resolution (roughly 4″) but with no intrinsic energy resolution, and with much lower sensitivity to diffuse X-ray emission than the IPC. In the central region of the detector the background was fairly spatially uniform. Two techniques were employed for estimating background in the Abell 2218 observation. In the first, the annular region 4′–6′ from the cluster center was fitted with a uniform background model assuming no cluster emission. Then the region within 4′ was modeled with both this background level (held fixed) and emission from an isothermal-β cluster model. The parameters of the cluster model were adjusted to obtain the best fit. The emission from this cluster model was extrapolated to the 4′–6′ annular region, and a new background estimate was made. This procedure was iterated until the change in background rate was less than the statistical uncertainty; in fact only a single iteration was necessary. The second technique estimated the background by examining the annular region from 8′ to 10′ and assuming it to be source free. Both techniques yielded consistent values for the background of $(5.20 \pm 0.05) \times 10^{-3}$ counts s^{-1} arcmin^{-2}. The resulting background-subtracted HRI image, smoothed by a Gaussian with $\sigma = 16''$ is shown in Figure 2*b*. Within a radius of 4′, the HRI count rate of the cluster is 0.0509 ± 0.0037 s^{-1} (1 σ error, including the background subtraction uncertainty).

These images of A2218 show a smooth, symmetric distribution of X-ray emission, with no evidence for a strong central point source or surface brightness spike, as might arise from the presence of a cooling flow. Our detailed fits, discussed below, confirm these qualitative impressions and allow us to demonstrate consistency between the two data sets.

2.3. *X-Ray Spectrum*

A *Ginga* X-ray spectrum of Abell 2218 has been observed and analyzed by McHardy et al. (1990). Since the large area counters (LAC) on board *Ginga* which produced this spectrum were insensitive to levels of interstellar absorption less than about several times 10^{21}, McHardy et al. fixed the absorption at the galactic value of 3×10^{20} cm^{-2} (Stark et al. 1984). Their analysis showed that the spectrum was consistent with an isothermal plasma model with

$$T_e = 6.7 \pm 0.45 \text{ keV} \quad (1)$$

$$\text{metallicity} = 0.2 \pm 0.2 \text{ solar} \quad (2)$$

for the intergalactic gas in Abell 2218, where we have replaced the errors on the estimate of the electron temperature T_e given by McHardy et al. (1990) by a symmetrical error bound. Results (1) and (2) are fully consistent with the independent analysis of the same *Ginga* data performed by Hatsukade (1989).

The result (1) for the temperature of the intracluster gas in Abell 2218 is sensitive to the uncertain background count rate in the *Ginga* LAC. McHardy et al. suggest that the largest plausible error in the background might cause the estimate of the electron temperature to be in error by about 2 keV. We will assume, therefore, that a systematic error at the level ± 1 keV (at ± 1 σ) might be present in equation (1). This is similar to the error caused by the uncertain background subtraction esti-

mated from the analysis of *Ginga* spectral data for Abell 665 (Hughes & Tanaka 1992), a cluster with a similar *Ginga* count rate to Abell 2218.

The *Einstein* IPC also produced an X-ray spectrum of the cluster, albeit over a lower energy band (0.2–4.0 keV) and with limited statistical precision. Because of the upper energy cutoff of the IPC band, this spectrum cannot provide a useful determination of the cluster temperature, but the lower energy band makes it useful for determining the line-of-sight absorbing column density, which is found to be

$$N_{\rm H} = 6.6^{+12.5}_{-4.7} \times 10^{20}\ {\rm cm}^{-2} \quad (3)$$

(with 90% errors) when we make use of the *Ginga* results for the temperature to specify the intrinsic spectrum of the cluster. The observed fluxes from the IPC and LAC for the spectral model given by (1), (2), and (3) are consistent to within the uncertainties of the background subtraction.

It was also possible to place a constraint on the absorbing column density from the ratio of IPC to HRI fluxes. Because the source is extended we could not simply take the ratio of observed count rates in the two instruments, but rather we compared the normalizations ($N_{\rm X}$) from our fits to the X-ray images for the same isothermal β-model (see § 3.2), taking account of the differing background subtraction and spatial resolution functions. The ratio of the IPC and HRI normalizations is 3.05 ± 0.26 where the error includes uncertainty due to background subtraction and a 5% error in the relative normalization of the instruments both added in quadrature to the statistical error, and is not sensitive to the particular values chosen for the structural parameters.

We calculated the expected IPC/HRI ratios for a range of column density values assuming the spectral parameters (1) and (2). When the predicted values are compared to the observed ratio we constrain the column density to a value

$$N_{\rm H} = 6.5^{+5.0}_{-3.0} \times 10^{20}\ {\rm cm}^{-2}\ , \quad (4)$$

where the (90%) errors have been increased to account for the uncertainty caused by the errors on T_e and metallicity, although for such high gas temperatures the ratio depends only weakly on these quantities.

Estimates (3) and (4) for the column density are not independent, so we are not justified in combining the results to reduce the errors. The best-fit values are consistent, so we will utilize the more precise result (4) in further analysis. This result indicates at about the 90% confidence level that the column density toward Abell 2218 is larger than the galactic value. Although we will not pursue further discussion of the astrophysical implications of this result (since it is not statistically significant), in § 4.1 we demonstrate its importance in determining the proper value and error range for the Hubble constant.

3. ANALYSIS

3.1. *Models for the Cluster Gas*

The analysis of these results to produce an estimate of the Hubble constant follows the analysis used for Abell 665 (Birkinshaw et al. 1991). That is, the X-ray image and the Sunyaev-Zel'dovich effect scan are fitted with the same isothermal β-model for the intracluster medium, and the results of these fits are used to calculate the normalizations of the models.

The isothermal β-model for the cluster gas is described by an electron density distributed with radius in the cluster as

$$n_e = n_{e0}\left(1 + \frac{r^2}{r_{\rm cx}^2}\right)^{-3/2\beta} \quad (5)$$

and a constant electron temperature $T_e = T_{e0}$. Note particularly the assumption here that the cluster gas is distributed spherically, and that the intracluster medium is not clumpy. It can be shown (e.g., Sarazin 1986) that this model for the intracluster medium leads to an X-ray surface brightness distribution of the form

$$b_{\rm X}(\theta) = N_{\rm X}\sqrt{\pi}\,\frac{\Gamma(3\beta - 1/2)}{\Gamma(3\beta)}\,\theta_{\rm cx}\left(1 + \frac{\theta^2}{\theta_{\rm cx}^2}\right)^{1/2-3\beta} \quad (6)$$

and a Sunyaev-Zel'dovich effect of the form

$$\Delta T_{\rm RJ}(\theta) = N_{\rm RJ}\sqrt{\pi}\,\frac{\Gamma[(3/2)\beta - (1/2)]}{\Gamma(3\beta)}\,\theta_{\rm cx}\left(1 + \frac{\theta^2}{\theta_{\rm cx}^2}\right)^{1/2-3/2\beta}\ , \quad (7)$$

where θ is the angle from the center of the cluster, $\theta_{\rm cx}$ is the angular equivalent of the core radius $r_{\rm cx}$, and $N_{\rm X}$ and $N_{\rm RJ}$ are normalization constants.

Fits to the X-ray surface brightness and the Sunyaev-Zel'dovich effect of a cluster can use equations (6) and (7) to estimate several structural parameters: the location of the center of the cluster in R.A. and declination (although it is clear that the one-dimensional scan in the Sunyaev-Zel'dovich effect will not produce any useful constraint on the R.A. position the cluster center), the angular core radius of the cluster, $\theta_{\rm cx}$, and the β-parameter that describes the concentration of the density profile. The two normalizations $N_{\rm X}$ and $N_{\rm RJ}$ can also be fitted from the data.

Birkinshaw et al. (1991) showed that the angular diameter distance of the cluster can be obtained from the normalizations $N_{\rm RJ}$ and $N_{\rm X}$ using

$$D_{\rm A} = \left(\frac{N_{\rm RJ}^2}{N_{\rm X}}\right)\left(\frac{m_e c^2}{k_{\rm B} T_{e0}}\right)^2 \frac{\Lambda_{e0}}{16\pi T_r^2 \sigma_{\rm T}^2 (1+z)^3}\ , \quad (8)$$

where Λ_{e0} is the X-ray spectral emissivity of the cluster gas (calculated over the emitted energy range appropriate to the energy range of the X-ray detector), $\sigma_{\rm T}$ is the Thomson scattering cross section, $k_{\rm B}$ is the Boltzmann constant, c is the speed of light, m_e is the electron mass, $z = 0.171$ is the redshift of the cluster gas, and $T_r = 2.74$ K (Mather et al. 1990) is the thermodynamic temperature of the microwave background radiation. In deducing equation (8) it has been assumed that the cluster is at rest in the Hubble flow, since any notion of the cluster can cause an additional contribution (with the same angular dependence as eq. [7]) to the Sunyaev-Zel'dovich effect (e.g., Rephaeli & Lahav 1991).

Fits to the data will be made based on equations (6) and (7), with the X-ray fit taken to be of primary importance since the two-dimensional X-ray image will provide far better structural information than will the one-dimensional (and noisier) Sunyaev-Zel'dovich effect scan. The results for the location of the center of the cluster, β, and $\theta_{\rm cx}$ from the X-ray fit are then used to demonstrate consistency with the Sunyaev-Zel'dovich effect scan, and the normalizations from the two sets of fits are used to calculate $D_{\rm A}$ and hence the value of the Hubble constant.

3.2. *Fits to the X-Ray Images*

The *Einstein* IPC and HRI images for Abell 2218 were fitted in the same way as was the IPC image of Abell 665 in Birkinshaw et al. (1991). That is, a maximum-likelihood estimator was used to find the best-fitting cluster center, β, θ_{cx}, and N_X and to generate confidence intervals for these parameters. Since maximum-likelihood estimators do not produce goodness-of-fit statistics, the quality of the fit that was obtained was estimated by applying the Kolmogoroff-Smirnov test to the cumulative distribution of counts in the image, and by making a χ^2 test of the best-fit radial distribution.

Good fits were found to both the IPC and the HRI X-ray images of Abell 2218, with consistent centers for the atmosphere: $16^h35^m42^s.8$, $+66°18'44''.5$ from the IPC fit, and $16^h35^m41^s.3$, $+66°18'28''.0$ from the HRI with statistical errors of about 10″ for each. Within the errors, these are consistent with the center of the galaxy distribution in the cluster $16^h35^m37^s \pm 12^s$, $66°18'30'' \pm 30''$, but are strongly inconsistent with the location of the cluster center in right ascension determined by Klein et al. (1991) from their Sunyaev-Zel'dovich effect data, $16^h35^m26^s$. (A fit to the X-ray data using the Klein et al. center for the cluster also produces values of β and r_{cx} which would be unusual for a cluster atmosphere, and which would cause a bad fit to the Sunyaev-Zel'dovich effect data of Fig. 1.)

Confidence-level contours for fits to the IPC data are shown in Figure 3: it can be seen that the best-fit model has $\beta = 0.65$ and $\theta_{cx} = 1'.0$. These results are not sensitive to variations in the background subtraction or to the region of the detector over which the fit was performed. Varying the background by $\pm 20\%$ (as outlined in § 2.2) changed the best-fit core radius by at most $\pm 0'.05$ while the value of β changed by ± 0.02. Decreasing the radius of the fitted region in the detector from the nominal value (of 16′) to 8′ reduced θ_{cx} by 0′.06 and β by 0.015. These values are much smaller than the statistical errors associated with the fits, of ($-0'.25$ to $+0'.33$) in θ_{cx} and of (-0.05 to $+0.09$) in β (90% confidence ranges).

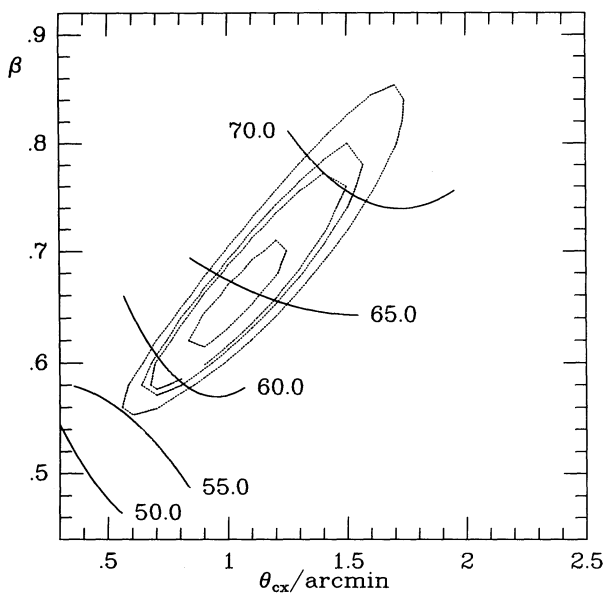

FIG. 3.—Confidence level contours for fits of isothermal β-models to the IPC image of Abell 2218, with superposed contours of the value of H_0 (in km s^{-1} Mpc^{-1}) derived from the X-ray and Sunyaev-Zel'dovich effect data. The best fit lies at $\beta = 0.65$, $\theta_{cx} = 1'.0$, and corresponds to $H_0 = 65$ km s^{-1} Mpc^{-1}. The random error at this point is 14 km s^{-1} Mpc^{-1}: when the systematic errors in the X-ray and Sunyaev-Zel'dovich effect data, and an error from the dependence of H_0 on the model values of β and θ_{cx}, are added in quadrature the overall error is increased to ± 25 km s^{-1} Mpc^{-1}.

We note that the derived core radius of the cluster is similar in value to the spatial resolution of the IPC, which has been modeled as a Gaussian with $\sigma = 36''$. In practice the spatial resolution of the IPC is energy dependent, and the value used corresponds to the on-axis spatial resolution of the IPC for pulse height channel 7 (Harnden et al. 1984), which is at the middle of the range of pulse height channels we accept. Over this range of pulse heights the variation in sigma is roughly 10%, which when used to fit the IPC data introduces an uncertainty of $\pm 0'.10$ in θ_{cx} and ± 0.015 in β. Again this systematic error is much smaller than the statistical error.

The fractional error on the X-ray normalization, N_X, including systematics due to background subtraction and the uncertain spatial resolution, is 7.6% (at 90% confidence), where the error is also dominated by the statistical uncertainty.

The left panel in Figure 4 shows a comparison between the best-fit model and the azimuthally averaged radial profile of the IPC data about the best-fit cluster center. The value of χ^2 from this comparison is 61.5 for 25 degrees of freedom. Most of the deviation comes from the last six data points where the background dominates the signal; excluding them reduces the χ^2 to 24.2 for 19 degrees of freedom. As mentioned above, our fits are not sensitive to reducing the radius of the fitting region by even as much as a factor of 2. The data and model extracted from separate quadrants of the image were also compared. There was no evidence for a deviation from azimuthal symmetry.

Although the HRI image of Abell 2218 contains far more counts than the IPC image, the determination of β and θ_{cx} based on the HRI data is much less precise than with the IPC. For nominal background subtraction (determined as discussed in § 2.2), fitting over the central 4′ radius of the cluster, we derive values of $\beta = 0.59$ (-0.10, $+0.16$) and $\theta_{cx} = 1'.00$ ($-0'.30$, $+0'.42$). These parameters are consistent with the results of the IPC fit at about the 90% confidence level. The right panel in Figure 4 shows the radially summed HRI data compared to the data: the corresponding value of χ^2 is 48.9 for 50 degrees of freedom. A comparison of the data and model in quadrants again shows no significant deviation from azimuthal symmetry. Note from Figure 4 the dominant effect of background on the HRI data: the structural parameters of the cluster derived from the HRI image are less certain than those based on the IPC image because the cluster emission is an appreciable fraction of the background to fewer core radii in the HRI data.

Fits based on the HRI data were somewhat sensitive to variations in the background subtraction and the region of the detector over which the fit was performed. Varying the background by $\pm 1.8\%$, which is the statistical error on the uniform background level, changed the best-fit core radius by ($-0'.11$, $+0'.07$) while the value of β changed by ± 0.06. Increasing the radius of the fitted region in the detector from the nominal value of 4′ to 8′ increased θ_{cx} by 0′.09 and β by 0.04. The spatial response of the HRI was modeled as a double exponential with scale lengths of 2″ and 12″ (Henry & Henriksen 1986). Errors in this response model introduce only insignificant variations in the fitted structural parameters of the cluster since the width of the point response function is much less than the angular size of the cluster.

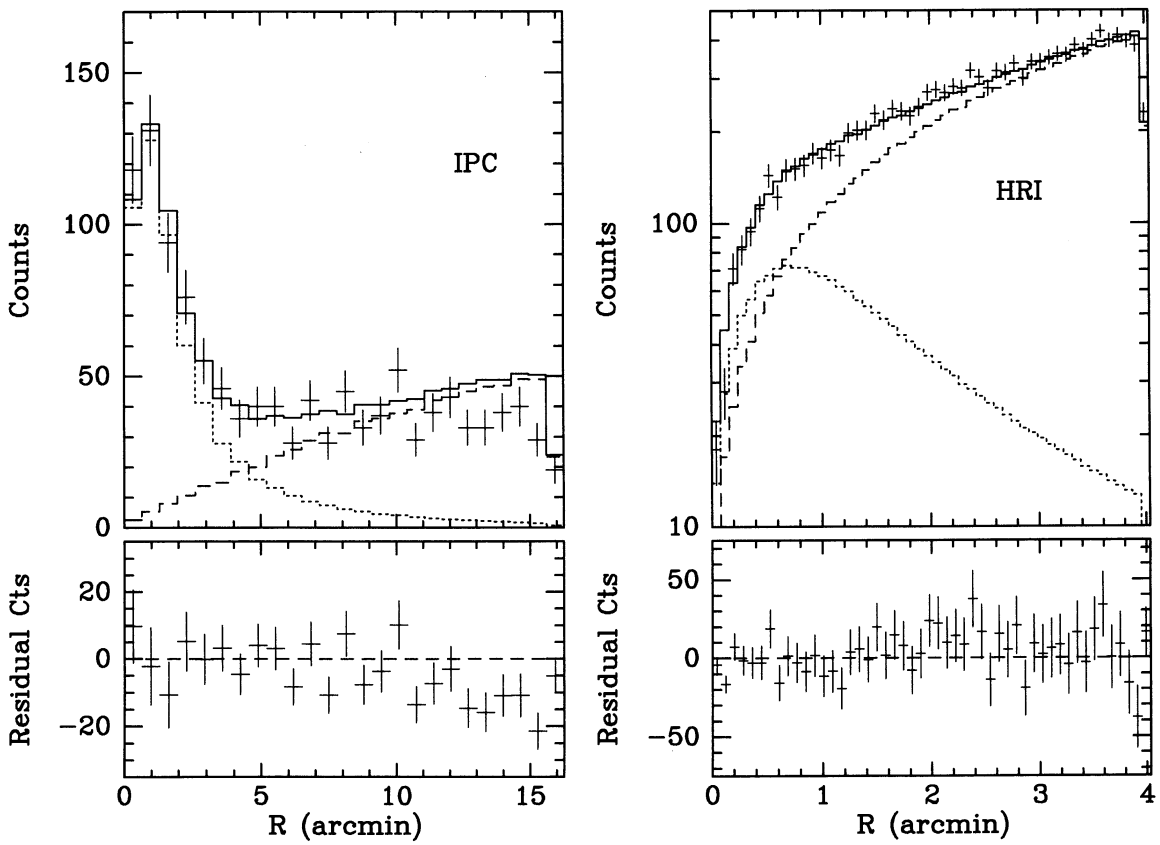

FIG. 4.—Comparisons of the radial X-ray profiles of the best-fitting isothermal β-model (with $\beta = 0.65$, $\theta_{cx} = 1'.0$) with the IPC and HRI radial profiles. The total numbers of counts in annular rings are shown vs. the distance from the center of the cluster. *Short dashed curves:* model cluster emission; *long dashed curves:* background; *solid curves:* sum of these. (*Left*) Comparison with the IPC. Note that the emission can be traced to about 7'. (*Right*) Comparison with the HRI. Note how the background dominates the cluster emission beyond about 0'.6.

The value of 0.65 derived for β is close to that found earlier for Abell 665 ($\beta = 0.66$; Birkinshaw et al. 1991), and is in the range that is normal for a rich X-ray cluster. Formally, however, $\beta = 0.65$ is not a permissible value, since it corresponds to $n_e \propto r^{-1.95}$ at large radius, and hence an infinite gas mass. This implies that some outer cutoff, r_{max} should be used for the model density distribution (5), but since the divergence is slow at large r, a large r_{max} cutoff ($r_{max} \gtrsim 10 r_{cx}$) will not have a significant effect on the shape of the X-ray or Sunyaev-Zel'dovich effect structures (eqs. [6] and [7]). However, there is some effect on the fitted normalizations, and hence the value of the Hubble constant, as discussed in § 4.2.

We fitted the IPC data with two independent isothermal β-models to search for evidence of substructure in the cluster. We tried a number of cases: (1) fixing the center of both components to the same position, (2) fixing θ_{cx} and β to the same values, and (3) letting free the positions and structural parameters of both models. In no case was a significant reduction in the likelihood parameter obtained.

We examined the HRI image for evidence of a point source near the cluster center which might indicate the presence of a strong cooling flow in the cluster core. An improved fit to these data was obtained when we included a point source in addition to the cluster model. The point source was located 5".4 west and 23".9 south of the cluster center with an intensity of 6.4×10^{-4} s^{-1}, about 1% of the count rate of the cluster. The 3 σ upper limit to the intensity of a point source near the cluster center is 1.3×10^{-3} s^{-1}. The inclusion of the point source resulted in a reduction in the likelihood parameter of 10, a value which indicates that the introduction of the three additional free parameters is statistically significant at about the 98% confidence level, but the influence of this source on the normalization of the β-model atmosphere, and hence on the derived Hubble constant, is negligible.

The X-ray normalization enters linearly into the value of the Hubble constant, so that its overall error (of $\pm 8\%$ at 90% confidence) is not the limiting factor in the accuracy of our final result. If the value of the Hubble constant is taken to be 50 km s^{-1} Mpc^{-1}, then the corresponding proton density at the cluster center is $n_{p0} = 5.4 \times 10^{-3}$ cm^{-3}: other assumptions for H_0 cause this value to vary as $H_0^{1/2}$.

3.3. *Fits to the Sunyaev-Zel'dovich Effect Scan*

Since the Sunyaev-Zel'dovich effect data exist at only seven points on a north-south line through the optical center of the cluster, they cannot be used to obtain good estimates of the structural parameters of the β-model atmosphere. In particular, no useful result on the R.A. of the cluster center is to be expected. After fixing the R.A. of the center of the atmosphere at $16^h35^m43^s$, as suggested by the IPC image, the scan can be used to fit β, θ_{cx}, N_{RJ}, and the declination of the cluster center. However, the small apparent angular size of the cluster (Fig. 1) indicates that only limits to the values of β and θ_{cx} can be obtained from such fits: effectively only the FWHM of the

cluster atmosphere, as sampled by the beam- and position-switching system of the 40 m telescope, can be estimated. However, the X-ray structural parameters $\beta = 0.65$, $\theta_{cx} = 1'.0$, are found to be consistent with the Sunyaev-Zel'dovich effect data, and lead to good fits. We therefore adopt these values of β and θ_{cx} in fitting the Sunyaev-Zel'dovich effect data for the declination of the cluster center and N_{RJ}.

The best-fit center of the atmosphere found under these assumptions lies at $+66°18'40'' \pm 20''$, consistent with both the X-ray and optical centers of the cluster, and this center produces a good fit to the data. Thus the simple isothermal β-model for the cluster atmosphere (5) appears to provide an adequate description of the gas in Abell 2218. The corresponding value of N_{RJ} implies that the central Sunyaev-Zel'dovich effect in Abell 2218 is -0.62 ± 0.08 mK. The observed central decrement of -0.43 mK (Table 1) thus reflects the $\sim 60\%$ efficiency of the 40 m telescope in observing the Sunyaev-Zel'dovich effect in a cluster at this redshift.

In performing this fit, account has been taken of all the individual point errors, ΔT_{syst}, in the Sunyaev-Zel'dovich effect data, of the apparent offset, ΔT_{zero}, in the overall zero level of the scan data, and of the factor 1.00 ± 0.06 scale error. The individual point systematic errors, ΔT_{syst}, were combined with the random errors in quadrature before the fits were performed. The zero level offset was taken into account by finding the variation in the results of the fits as ΔT_{zero} changes, and the overall scale factor produces a final multiplicative error on the results of the fits. The overall result for N_{RJ} found in the Sunyaev-Zel'dovich effect fits carries an error of 13%: from equation (8) we see that this will produce an error $\approx 25\%$ in the resulting estimate for the Hubble constant. Thus the uncertainties in the Sunyaev-Zel'dovich effect (which are dominated by those in the zero level and the scale error) are a major source of error in the estimate for the Hubble constant.

3.4. *The Value of the Hubble Constant*

Since the X-ray and Sunyaev-Zel'dovich effect data are consistent with the same, simple, spherical, isothermal, model for the gas in Abell 2218, the normalizations found in §§ 3.2 and 3.3 can be used to calculate the Hubble constant, with the assistance of equation (8). The results of this calculation are shown in Figure 3, where contours of constant H_0 appear superposed on the confidence level contours for β and θ_{cx} found from the X-ray fit.

The best-fitting model on Figure 3 has $H_0 = 65 \pm 19$ km s^{-1} Mpc^{-1}, where the error has been calculated from the error in N_{RJ}, including both random and systematic components, and the error in N_X, including random and systematic errors, but using only the result (1) from McHardy et al. (1990) for the temperature of the gas. If account is taken of the possible ± 1 keV systematic error in T_{e0} (§ 2.3), and of the dependence of the result for the Hubble constant on the values of the structural parameters β and θ_{cx} (Fig. 3), the overall result from this calculation is

$$H_0 = 65 \pm 25 \text{ km s}^{-1} \text{ Mpc}^{-1} . \quad (9)$$

In this result, approximately ± 15 km s^{-1} Mpc^{-1} of the error can be attributed directly to the systematic errors in N_{RJ} (principally from the zero level and gain errors), ± 3 km s^{-1} Mpc^{-1} can be attributed to the systematic errors in N_X, and ± 15 km s^{-1} Mpc^{-1} can be attributed to the ± 1 keV systematic error in T_{e0}. Clearly improvements in the estimate (9) require further work on the Sunyaev-Zel'dovich effect data, and on the X-ray spectrum of the cluster.

4. DISCUSSION

4.1. *Comparison with the Results of McHardy et al.*

The result (9) for the Hubble constant should be compared with McHardy et al. (1990)'s estimate

$$H_0 = 24^{+23}_{-10} \text{ km s}^{-1} \text{ Mpc}^{-1} \quad (10)$$

based on the same method for the same cluster. The discrepancy between our result (9) and McHardy et al.'s result (10) is serious and requires explanation if this method of deriving the value of the Hubble constant is to prove useful. A close examination of the two distinct calculations indicates that the difference between equations (9) and (10) consists of several parts:

(1) The differences in the model used for the electron density, n_e, as derived from the HRI data by McHardy et al., or from the IPC and HRI data in the present paper,

(2) McHardy et al.'s use of the Stark et al. (1984) value for the neutral hydrogen column density toward the cluster, which we find (§ 3.2) to be somewhat too low; and

(3) McHardy et al.'s use of an inconsistent description of the gas in comparing the X-ray surface brightness profile and the Sunyaev-Zel'dovich effect.

McHardy et al. derived the electron density in Abell 2218 based only on the HRI image. Figure 4 has demonstrated that these data are dominated by the background, so that small variations in the background subtraction will lead to large changes in the apparent structure of the X-ray emission from the cluster. No details of the background subtraction techniques are contained in McHardy et al.'s paper, so that our comparison of their results with ours are based solely on the derived density distributions.

The electron density model derived by McHardy et al. (1990) from the *Einstein* HRI data corresponds roughly to an isothermal-β model with $\beta = 0.5$ and $\theta_{cx} = 0'.6$, which is formally unacceptable from our fits to the IPC data. However, because of the low sensitivity of the HRI to extended X-ray emission (Fig. 4), McHardy et al. were unable to trace this X-ray emission beyond about 3′ from the cluster center, so that they have no direct information on the outer part of the cluster atmosphere. This is important because about 25% of the total electron pressure integral (which appears in the expression for the Sunyaev-Zel'dovich effect from the cluster) originates in gas lying between 3′ and 10′ from the cluster center, where McHardy et al.'s extrapolation of the electron density distribution is unsupported by their X-ray data. Since the derived value of the Hubble constant depends on the square of the pressure integral (eq. [8]), this part of the cluster atmosphere contributes almost 60% of the value of the Hubble constant (10). By contrast, the approach of using the IPC data, followed in the present paper, allows the gas density profile to be traced out to a radius $\gtrsim 7'$. About 90% of the line-of-sight electron pressure integral arises from gas within this radius (if the electron distribution is assumed to extend to infinity), while 97% of the pressure integral within 10′ is produced by gas whose distribution is directly sampled in the X-ray surface brightness profile (Fig. 4). The different structural models for the cluster used in the present paper and by McHardy et al. produces the largest single contribution to the discrepancy between results (9) and (10) for H_0: we find that McHardy et al.'s estimate of the line-of-sight integral of the electron pressure is about 31% less than our value.

An additional component of the discrepancy in the values of H_0 originates in McHardy et al.'s assumption that the column density to the cluster is given by the Stark et al. (1984) value. We have shown (§ 3.2) that this value is at the lower limit of acceptable values, as determined by fits to the low-energy X-ray spectrum. Since the HRI has no intrinsic energy resolution, and includes counts from X-ray photons with energies as low as 0.1 keV, the count rate measured using the HRI is more sensitive to the absorbing column density than is the count rate measured using the IPC. Furthermore, in our present analysis we have been able to use the intrinsic energy resolution of the IPC to perform our analysis using only counts corresponding to photon energies above 0.8 keV, where variations in the absorbing column have little effect on our results. The effect of McHardy et al.'s choice of the Stark et al. (1984) column toward Abell 2218 causes their integrated electron pressure to be underestimated by about 12%.

Combining these two effects, we can show that McHardy et al.'s estimate of the electron pressure integral (or, equivalently, any fiducial electron density in the cluster) will be about 48% smaller than our value. Since the value of the Hubble constant is proportional to the square of this pressure integral, we would expect McHardy et al.'s estimate of the Hubble constant to be too low by a factor of 2.1. This difference explains most of the discrepancy between the results (9) and (10).

The remaining part of the discrepancy comes from the normalization of the Sunyaev-Zel'dovich effect. Our present normalization is equivalent to a central Sunyaev-Zel'dovich effect of $\Delta T_0 = -0.62 \pm 0.08$ mK in Abell 2218, where this value was determined by fitting the same model atmosphere (with $\beta = 0.65$ and $\theta_{cx} = 1'.0$; § 3.1) that produces a good fit to the X-ray surface brightness. However, the normalization used by McHardy et al., $\Delta T_0 = -0.69 \pm 0.10$ mK, was based on a fit by Birkinshaw (1987) to earlier Sunyaev-Zel'dovich effect data using models with $\beta = 0.5$ and $\theta_{cx} < 1'$. This earlier value for the normalization is therefore based on a density model that is consistent with neither the model atmosphere derived from our present analysis of the X-ray structure of the cluster, nor with the model atmosphere of McHardy et al., and we would not expect the use of this earlier normalization to produce a useful estimate of the Hubble constant. Thus McHardy et al.'s use of the normalization $\Delta T_0 = -0.69 \pm 0.10$ mK produces a further error in their estimate for H_0: we find that the McHardy et al. result would be an underestimate by a further 23%.

Combining all three factors, we calculate that the McHardy et al. result (10) is too low by a factor of about 2.6, because it was derived using an incorrect electron number density distribution and inconsistent models for the X-ray and Sunyaev-Zel'dovich effect data. If the result (10) is corrected by this factor, the result is consistent with our result (9).

4.2. *The Model Dependence of the Value for the Hubble Constant*

In calculating the result (9) for the value of the Hubble constant, we have already included a systematic error (of ± 7 km s^{-1} Mpc^{-1} in quadrature) based on the dependence of our estimate for H_0 on the parameters of the isothermal β models that we use to fit the X-ray emission. However, the choice of isothermal β models to describe the atmosphere of the cluster does not exhaust the list of plausible structures that the atmosphere might adopt—in particular, it restricts the thermal structure of the atmosphere to a simple form that is not consistent with the more complicated structures seen in some nearby clusters (e.g., the Coma cluster; Hughes et al. 1993). Thus it is of interest to examine the effect that qualitative variations of the model atmosphere have on the estimate for H_0.

In order to assess these effects, we have chosen to modify the isothermal β model (5) by incorporating an outer density cutoff (so that $n_e = 0$ at $r > r_{max}$), and by allowing the temperature to assume a polytropic dependence on density (with the polytropic index chosen to be the maximum value consistent with a physical cluster potential holding a β-model atmosphere in hydrostatic equilibrium, $\gamma = 1 + (1/3\beta) = 1.51$; Hughes et al. 1988) outside an isothermal region of radius r_{iso}. We chose several values of r_{iso}/r_{cx} and r_{max}/r_{cx}, and fitted the X-ray surface brightness and the X-ray spectrum of Abell 2218 self-consistently using these models to produce estimates of the temperature of the gas in the isothermal core of the cluster and the X-ray surface brightness normalization. Values of the Sunyaev-Zel'dovich normalization fitted using these same models were also calculated from the scan data (Table 1), and these normalizations and temperatures were then combined to produce further estimates for the Hubble constant.

If the isothermal radius is much larger than the core radius, then the results of § 3 are little altered: values of the Hubble constant which differ by less than 10% from (9) are obtained for $r_{iso} \gtrsim 10 r_{cx}$. If the isothermal radius is only a few r_{cx}, however, substantially larger values of the Hubble constant are obtained—for $r_{iso} \approx 4 r_{cx}$, the best-fitting models have values of $H_0 \approx 80$ km s^{-1} Mpc^{-1}. The increase in the apparent Hubble constant arises mostly from the different central electron temperatures required in the cluster for a good fit to both the spectrum and the surface brightness profile: the result for the Hubble constant scales approximately as T_{e0}^2, and the central electron temperature is about 10% higher for these models than for wholly isothermal models.

We conclude, therefore, that it is possible that the result (9) for the Hubble constant is an underestimate if Abell 2218 displays an outer polytropic temperature profile. However, the changes in the Hubble constant that are produced are comparable with the systematic error caused by the ± 1 keV systematic error in the temperature deduced from the *Ginga* spectrum: a more precise determination of the X-ray spectrum of Abell 2218 would provide stronger constraints on thermal structure in the cluster and produce a substantial reduction in the T_e-based systematic error on the estimate of the Hubble constant (9).

The position offset of $\sim 1'.5$ between the center of the cluster as determined from the X-ray image and from the Klein et al. (1991) Sunyaev-Zel'dovich effect data (see § 3.2) was interpreted by Klein et al. as a possible indication of a complicated density and thermal structure in Abell 2218. If real, a major feature in the cluster atmosphere, with the unusual property of producing a large Sunyaev-Zel'dovich effect but little X-ray emission, is implied by the Klein et al. position shift: on the basis of the model atmosphere that best fits the *Einstein* IPC and HRI data, Klein et al. should have detected only about 10% of the peak Sunyaev-Zel'dovich effect at their center, and no indication of a corresponding X-ray feature can be found in the HRI image (Fig. 2*b*). If the complicated structure implied by the Klein et al. result is present in Abell 2218, then far more detailed X-ray and Sunyaev-Zel'dovich effect mapping of the cluster is needed if the present method is to be used to derive the Hubble constant. However, the Klein et al. data have low significance (they measured an effect of -0.6 ± 0.2 mK), so that the evidence for a major structural feature in the cluster

atmosphere that would invalidate the derived value of the Hubble constant (eq. [9]) is weak.

4.3. *The Overall Value for the Hubble Constant*

The present result for the Hubble constant can be compared with the result obtained from Abell 665 (Birkinshaw et al. 1991), to discover whether this method of determining H_0 produces consistent results, and hence whether there are substantial unknown variations in the properties of the cluster atmospheres (for example, in strongly varying clumping in the gas, or dramatic thermal structures) that cause large scatter in the Hubble constant values.

Birkinshaw et al. used data for Abell 665 to find $H_0 = 45 \pm 13$ km s^{-1} Mpc^{-1}, where we have taken the error range quoted in that paper and converted it into a $\pm 1\,\sigma$ error. This result has been updated by Birkinshaw et al. (1993), who used the full available Sunyaev-Zel'dovich effect data set, and a more conservative set of systematic error estimates, to obtain $H_0 = 51 \pm 18$ km s^{-1} Mpc^{-1}. For Abell 2218, we have shown in § 3 that $H_0 = 65 \pm 25$ km s^{-1} Mpc^{-1}, from which we deduce an average value for the Hubble constant, based on the two clusters taken together, of

$$H_0 = 55 \pm 17 \text{ km s}^{-1} \text{ Mpc}^{-1}\,, \qquad (11)$$

where the error sum has taken account of the fully correlated errors in the two estimates produced by the uncertainty in the sensitivity of the 40 m telescope.

The consistency of the results for the Hubble constant based upon two different clusters suggests that this method is fairly robust, although the errors in the Hubble constant values are still large. In gaining the estimates based on clusters Abell 665 and 2218 we ignored the effects of clumping in the intracluster medium (which could cause these values of the Hubble constant to be overestimates, if the clumping is isobaric), we assumed that the clusters were at rest in the Hubble flow, we ignored any thermal structure in the clusters (the gas is assumed to be isothermal), any large-scale substructure in the clusters was also ignored, it was assumed that the clusters were spherical, and it was implicitly assumed that the somewhat different gas that contributes to the X-ray surface brightness (dominated by gas in the cluster cores) and the Sunyaev-Zel'dovich effect (dominated by gas further out in the clusters) can be related by a smooth density law of the form (5). Since the two clusters Abell 665 and Abell 2218 now produce similar estimates for the Hubble constant, it appears that these assumptions are either valid, or invalid in similar ways, in the two clusters: thus, for example, if both clusters contain isothermal cores and polytropic halos of the type considered in § 4.2, the value of the Hubble constant (11) may be underestimated by 20%–30%.

Since these data are subject to a selection effect, that elongated clusters are more readily detected if they are elongated along the line-of-sight, it could still be true that similar biases in the derived value of H_0 are present in the two clusters, causing perhaps a factor 1.5 or 2 decrease in the reported value of the Hubble constant (11) from its true value (see the discussion in Birkinshaw et al. 1991). In order to eliminate this selection effect, it will be necessary to repeat this process of deducing the Hubble constant using a number of clusters selected in a way that is not biased by their surface brightnesses—for example, by selecting clusters on the basis of their total X-ray densities.

For most of the other assumptions that are necessary to derive the value of the Hubble constant there is little reason to suspect similar effects in different clusters. Thus, for example, the clumping of the intracluster medium is either weak (and hence has little effect on the estimate of the Hubble constant), or is strong, and should vary substantially according to the detailed structure of the clusters, producing large variations in the apparent Hubble constant. No such effect is seen at the $\sim 30\%$ level implied by the consistency of the results for Abell 665 and 2218. Similarly, large-scale thermal structure in clusters, or substructure in the gas caused by substructure in the clusters, might not be expected to be the same, and could have an effect at the 50% level on the value of the Hubble constant, but such large variations are not present.

Thus the agreement of the estimates for the Hubble constant based on clusters Abell 665 and 2218, which leads to the overall estimate (11), argues that if these results are strongly affected by selection effects or other biases, then those biases are similar in these two clusters. The best test of the presence or otherwise of these biases would be to repeat this procedure, measuring the Sunyaev-Zel'dovich effects and X-ray properties of more clusters, and then calculating a larger set of estimates of the Hubble constant.

5. CONCLUSIONS

The conclusions of this paper can be summarized as follows:

(1) The structure of the intracluster medium in Abell 2218 is well described by a spherical, isothermal β-model with $\beta \approx 0.65$ and $\theta_{cx} \approx 1'.0$ centered at the optical center of the cluster;

(2) The value of the Hubble constant implied from these data for Abell 2218 is

$$H_0 = 65 \pm 25 \text{ km s}^{-1} \text{ Mpc}^{-1}\,; \qquad (12)$$

(3) McHardy et al. (1990)'s estimate of $H_0 = 24^{+23}_{-10}$ km s^{-1} Mpc^{-1}, based on the X-ray and Sunyaev-Zel'dovich effect data for Abell 2218 appears to be in error principally because of their use of the HRI data to obtain the electron density profile, and their use of an inconsistent description of the cluster gas in fitting the X-ray and Sunyaev-Zel'dovich effect data; and

(4) Combining the present result for the Hubble constant with that obtained earlier for Abell 665, we find an overall result

$$H_0 = 55 \pm 17 \text{ km s}^{-1} \text{ Mpc}^{-1}\,. \qquad (13)$$

Further work on the estimation of the value of the Hubble constant by this method should attempt to produce better-quality X-ray spectra of the clusters that might constrain their thermal structure, and must work to reduce the systematic errors in the Sunyaev-Zel'dovich effect measurements: both factors make an appreciable contribution to the large errors in equations (12) and (13) above. Better structural data for clusters could reduce the qualitative uncertainty in the choice of models and would also be valuable: thus *ROSAT* PSPC data on Abell 2218 (which are not yet available to us) will restrict the set of permissible models of the gas distribution through the improved angular and spectral resolution compared to the *Einstein* IPC data.

This research was supported by NSF grant AST 90-05038, NASA grants NAG 8-699 and NAG 8-181, and NASA contract NAS 5-30934.

REFERENCES

Abell, G. O. 1958, ApJS, 3, 311
Birkinshaw, M. 1979, MNRAS, 187, 847
———. 1987, in NRAO GreenBank Workshop 16, ed. C. O'Dea & J. Uson (Green Bank, WV: NRAO), 261
———. 1990, The Cosmic Microwave Background: 25 Years Later, ed. N. Mandolesi & N. Vittorio (Dordrecht: Kluwer), 77
Birkinshaw, M., Gull, S. F., & Hardebeck, H. 1984, Nature, 309, 34
Birkinshaw, M., Gull, S. F., Hardebeck, H. E., & Moffet, A. T. 1993, ApJ, submitted
Birkinshaw, M., Hughes, J. P., & Arnaud, K. A. 1991, ApJ, 379, 466
Cavaliere, A., Danese, L., & De Zotti, G. 1979, A&A, 75, 322
Dressler, A. 1978a, ApJ, 223, 765
———. 1978b, ApJ, 226, 55
Gunn, J. E. 1978, in Observational Cosmology, 1, ed. A. Maeder, L. Martinet & G. Tammann (Sauverny: Geneva Obs.)
Harnden, F. R., Jr., Fabricant, D. G., Harris, D. E., & Schwarz, J. 1984, Scientific Specification of the Data Analysis System for the Einstein Observatory Imaging Proportional Counter (SAO Special Report 393), 22
Hatsukade, I. 1989, Ph.D. thesis, Osaka University
Henry, J. P., & Henriksen, M. J. 1986, ApJ, 301, 689
Hughes, J. P., Butcher, J. A., Stewart, G. C., & Tanaka, Y. 1993, ApJ, 404, 611
Hughes, J. P., & Tanaka, Y. 1992, ApJ, 398, 62
Hughes, J. P., Yamashita, K., Okumura, Y., Tsunemi, H., & Matsuoka, M. 1988, ApJ, 327, 615
Klein, U., Rephaeli, Y., Schlickeiser, R., & Wielebinski, R. 1991, A&A, 244, 43
Mather, J. C., et al. 1990, ApJ, 354, L37
McHardy, I. M., Stewart, G. C., Edge, A. C., Cooke, B. A., Yamashita, K., & Hatsukade, I. 1990, MNRAS, 242, 215
Moffet, A. T., & Birkinshaw, M. 1989, AJ, 98, 1148
Rephaeli, Y., & Lahav, O. 1991, ApJ, 372, 21
Sarazin, C. L. 1986, Rev. Mod. Phys., 58, 1
Silk, J. I., & White, S. D. M. 1978, ApJ, 226, L103
Stark, A. A., Heiles, C., Bally, J., & Linke, R. 1984, privately distributed magnetic tape
Turner, E. L., Cen, R., & Ostriker, J. P. 1992, AJ, 103, 1427
Uson, J. 1987, in Radio Continuum Processes in Clusters of Galaxies, NRAO GreenBank Workshop 16, ed. C. O'Dea & J. Uson (Green Bank, WV), 255